A Density Functional Theory Study on the Mechanism of the Permanganate Oxidation of Substituted Alkenes

Th. Strassner* and M. Busold

Technical University Munich, Department of Inorganic Chemistry, Lichtenbergstrasse 4, D-85747 Garching, Germany

thomas.strassner@ch.tum.de

Received April 17, 2000

Oxidation of substituted alkenes by permanganate follows a (3 + 2) cycloaddition mechanism. DFT calculations (Becke3LYP/6-31G(d)) strongly favor the (3 + 2) pathway against a (2 + 2) pathway that proceeds through a metallaoxetane. The difference in free activation energy between the two pathways is around 40 to 45 kcal/mol for the nine compounds covered. The results for the (3 + 2) cycloaddition mechanism are in agreement with experimentally observed kinetic data reported earlier. Symmetric transition states are calculated for alkenes with at least one CH_2 group between the double bond and the acid group, while all others are unsymmetrical due to the repulsion between the permanganate oxygens and the carboxylic oxygens. Steric bulk, introduced by the number and position of substituents at the double bond, has no significant effect on the activation energies. A higher level of theory (Becke3LYP/6-311G(d,p)) leads to a reduction of the rmsd between experimental and calculated values, but has little influence on the calculated geometries.

The oxidation of alkenes by permanganate is one of the frequently used examples in freshman chemistry. There are many reagents that add two OH groups to a double bond,[1] but osmium tetraoxide and permanganate are the most prominent ones. The mechanism of the permanganate oxidation is believed to be similar to the oxidation of alkenes by OsO_4.[2]

It was generally accepted that the reaction proceeds via a concerted mechanism with a cyclic ester intermediate, until the suggestion was made of a stepwise mechanism involving a metallaoxetane intermediate.[3]

Scheme 1 shows the two proposed pathways. The stepwise mechanism proceeds via a (2 + 2) transition state (TS) and a metallaoxetane ((2 + 2) product) which is supposed to rearrange to a cyclic ester ((3 + 2) product) before the hydrolysis takes place, while the textbook mechanism via the (3 + 2) transition state is expected to lead directly to the (3 + 2) product. Hydrolysis of the intermediate is generally accepted to give rise to the observed diols.

Several groups started investigations to identify the elusive metallaoxetane, and a wealth of kinetic data provided no indication for the existence of the species. But the possibility that it might be a non-rate-determining intermediate could not be excluded. Different mechanisms were proposed[4] to explain the variety of experimental results available, but the mechanistic issues remained unresolved.

Since the introduction of density functional theory, theoretical calculations have been very successful in calculating structures and energies of organometallic compounds. An emerging competency is the treatment of complex reactions, where a critical element is the ability to directly model the transition state.

Scheme 1. (3 + 2) and (2 + 2) Reaction Pathways

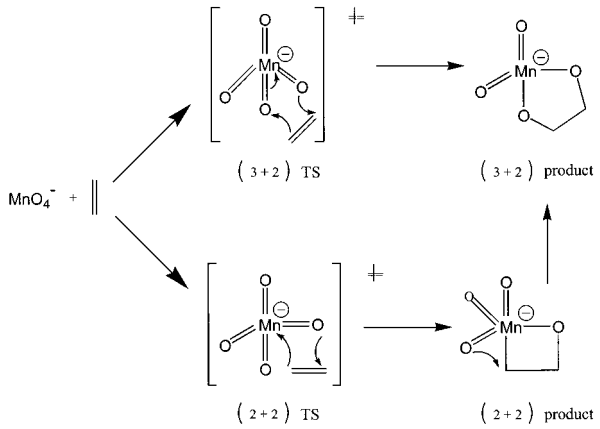

Knowledge of the structures and relative energies of possible transition states can be helpful in pointing the way to the correct mechanism.[5] Especially in combination with experimental observation, theory can provide valuable insight into the reaction mechanism.

Those observations might be isotope effects as they have been used before to study the oxidation of alkenes[6] or approximate free energy values. Experimental work often provides a $\Delta G^{\ddagger}$ value for the rate-determining

(1) For reviews see Sheldon, R. A.; Kochi, J. K. *Metal-Catalyzed Oxidations of Organic Compounds*; Academic Press: New York, 1981; pp 162−171, 294−296.

(2) (a) Waters, W. A. *Quart. Rev.* **1958**, *12*, 29. (b) Henbest, H. B.; Jackson, W. R.; Robb, B. C. G. *J. Chem. Soc. B* **1966**, 803.

(3) Sharpless, K. B.; Teranishi, A. Y.; Bäckvall, J. E. *J. Am. Chem. Soc.* **1977**, *99*, 3120.

(4) (a) Wolfe, S.; Ingold, C. F.; Lemieux, R. U. *J. Am. Chem.* Soc. **1981**, *103*, 938. (b) Simándi, L. I.; Jáky, M. *J. Am. Chem. Soc.* **1976**, *98*, 1995.

(5) Pidun, U.; Boehme, C.; Frenking, G. *Angew. Chem., Int. Ed. Engl.* **1996**, *35*, 2817. (b) Dapprich, S.; Ujaque, G.; Maseras, F.; Lledos, A.; Musaev, D. G.; Morokuma, K. *J. Am. Chem. Soc.* **1996**, *118*, 11660. (c) Torrent, M.; Deng, L.; Duran, M.; Sola, M.; Ziegler T. *Organometallics* **1997**, *1*, 13.

(6) (a) DelMonte, A. J.; Haller, J.; Houk, K. N.; Sharpless, K. B.; Singleton, D. A.; Strassner, Th.; Thomas, A. A. *J. Am. Chem. Soc.* **1997**, *119*, 9907. (b) Strassner, Th., Houk, K. N. *J. Org. Chem.* **1999**, *64*, 800.

10.1021/jo000575e CCC: $20.00
Published on Web 01/11/2001

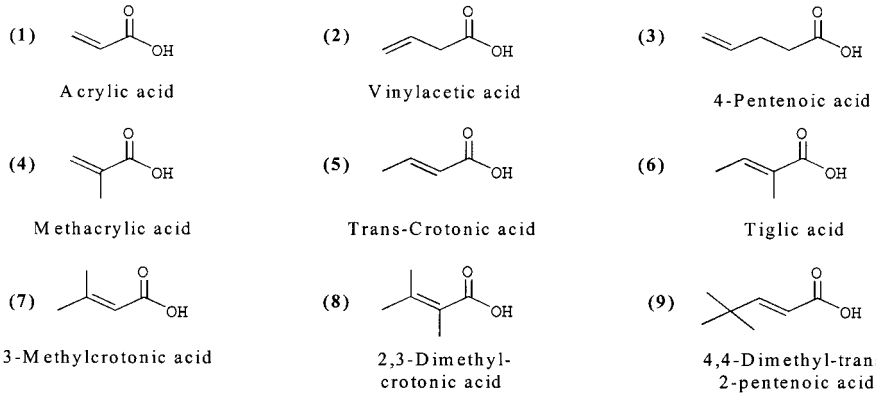

Figure 1. Unsaturated carboxylic acids **1**−**9** used in this study.

Table 1. Calculated (BS1) Free Energies for the Ground and Transition States for Both Pathways, Solvation Energies for the Transition States, and Experimental Data for Compounds 1−9 (in kcal/mol)

compound	$\Delta G^{\ddagger}_{exp}$	$\Delta G^{\ddagger}$ (3 + 2) TS	$\Delta G^{\ddagger}$ (2 + 2) TS	$\Delta G^{\ddagger}$ (3 + 2) TS PCM	$\Delta G^{\ddagger}$ (2 + 2) TS PCM	ΔG (3 + 2) GS	ΔG (2 + 2) GS
1	17.1	10.8	53.6	15.4	52.6	−35.3	26.8
2	17.8	17.7	58.0	15.0	61.4	−37.8	25.0
3	17.6	17.2	56.1	16.3	54.4	−38.1	24.7
4	17.1	11.8	55.1	16.2	54.1	−34.5	27.7
5	17.4	12.7	57.2	17.3	53.5	−32.9	29.8
6	17.0	13.5	57.5	15.5	54.3	−32.6	29.7
7	18.3	14.7	59.4	17.4	57.4	−30.0	33.6
8	18.6	14.6	58.9	20.6	61.4	−35.7	32.5
9	18.0	11.9	57.4	17.0	55.5	−33.9	30.8

transition state, but assigning a certain structure from experimental data is difficult. Quantum chemical calculations can provide those structures and the corresponding energies.

Here we present a study of unsaturated carboxylic acids (Figure 1) comparing calculated $\Delta G^{\ddagger}$ values of possible transition states with free energy values derived from experimental kinetic data.[7a]

Freeman and Kappos[7a] studied the influence of substituents on the rate of the permanganate oxidation in phosphate-buffered solutions (pH 6.83 ± 0.03). Nine unsaturated carboxylic acids have been used as substrates (Figure 1).

In compounds **1** to **3** the chain length and position of the double bond is varied, while compounds **4** to **9** are all α,β-unsaturated carboxylic acids with a changing number and position of alkyl substituents at the double bond. The rates of reaction were measured by monitoring spectral changes with a stopped flow spectrometer. Using pseudo-first-order conditions, they recorded the disappearance of the permanganate ion at 526, 584, or 660 nm and/or the rate of formation of colloidal manganese dioxide at 418 nm. The authors concluded that according to the measured reaction rates, the rate of oxidation is more sensitive to steric factors than to electronic effects. Regarding the reaction mechanism, they suggested that both the (3 + 2) and the (2 + 2) transition state are in agreement with their results.

The systematic experimental study was designed to measure the kinetics at standardized conditions and constant temperature (T = 298 K). Therefore, only the free energy of activation could be calculated from the experimental rate constant via the theory of the activated complex.[7b,c] The experimental $\Delta G^{\ddagger}$ values were obtained according to the following equation:

$$k = \frac{k_c \cdot T}{h} \cdot e^{\frac{-\Delta G^{\ddagger}}{RT}}$$

The density functional/Hartree−Fock hybrid model Becke3LYP [8,9] as implemented in GAUSSIAN 98[10] has been used throughout this study. Two different basis sets have been employed in the DFT calculations: the split valence double-ζ (DZ) basis set 6-31G(d) with a triple-ζ (TZ)[11] valence basis set for manganese (we will refer to this combination as basis set I (**BS1**)) and the triple-ζ basis set 6-311+G(d,p), which will be denoted as basis set II (**BS2**). All geometries have been fully optimized and frequency calculations ensured that they either correspond to minima (NIMAG 0) or transition states (NIMAG 1) on the potential energy surface. All energies listed are ZPE corrected and are given in kcal/mol relative to the reactands. All values are unscaled, the stability of the wave function was checked and unrestricted calculations ensured that no radical intermediates have to be considered. The solvent model used is Tomasi's PCM model as implemented in GAUSSIAN 98.[10]

(7) (a) Freeman, F.; Kappos J. C. *J. Org. Chem.* **1986**, *51*, 1654. (b) *Transition State Modeling for Catalysis*; Truhlar, D. G., Morokuma, K., Eds.; ACS Symposium Series 721; American Chemical Society: Washington, DC, 1999. (c) Cox, B. G. *Modern Liquid-Phase Kinetics*; Oxford University Press: Oxford, 1994; p 45.

(8) Lee, C.; Yang, W.; Parr, R. G. *Phys. Rev. B* **1988**, *37*, 785.

(9) (a) Becke, A. D. *J. Chem. Phys.* **1992**, *97*, 9173. (b) Becke, A. D. *J. Chem. Phys.* **1993**, *98*, 1372. (c) Becke, A. D. *J. Chem. Phys.* **1993**, *98*, 5648.

(10) M. J. Frisch, G. W. Trucks, H. B. Schlegel, G. E. Scuseria, M. A. Robb, J. R. Cheeseman, V. G. Zakrzewski, J. A. Montgomery, Jr., R. E. Stratmann, J. C. Burant, S. Dapprich, J. M. Millam, A. D. Daniels, K. N. Kudin, M. C. Strain, O. Farkas, J. Tomasi, V. Barone, M. Cossi, R. Cammi, B. Mennucci, C. Pomelli, C. Adamo, S. Clifford, J. Ochterski, G. A. Petersson, P. Y. Ayala, Q. Cui, K. Morokuma, D. K. Malick, A. D. Rabuck, K. Raghavachari, J. B. Foresman, J. Cioslowski, J. V. Ortiz, B. B. Stefanov, G. Liu, A. Liashenko, P. Piskorz, I. Komaromi, R. Gomperts, R. L. Martin, D. J. Fox, T. Keith, M. A. Al-Laham, C. Y. Peng, A. Nanayakkara, C. Gonzalez, M. Challacombe, P. M. W. Gill, B. Johnson, W. Chen, M. W. Wong, J. L. Andres, C. Gonzalez, M. Head-Gordon, E. S. Replogle, and J. A. Pople. *Gaussian 98, Revision A.7*, Gaussian, Inc.: Pittsburgh, PA, 1998.

(11) Schäfer, A.; Huber, C.; Ahlrichs, R. *J. Chem. Phys.* **1994**, *100*, 5829.

Table 2: Free Activation Energies for the (3 + 2) and (2 + 2) Transition States Calculated with Basis Sets BS1 and BS2

compd	$\Delta G^{\ddagger}_{exp}$	$\Delta G^{\ddagger}$ (3 + 2) TS BS2	$\Delta G^{\ddagger}$ (3 + 2) TS BS1	$\Delta G^{\ddagger}$ (2 + 2) TS BS2	$\Delta G^{\ddagger}$ (2 + 2) TS BS1
1	17.1	15.7	10.8	61.5	53.6
2	17.8	22.0	17.7	63.4	58.0
3	17.6	21.3	17.2	62.0	56.1
4	17.1	18.3	11.8	63.7	55.1
5	17.4	18.3	12.7	64.8	57.2
6	17.0	19.6	13.5	65.9	57.5
7	18.3	21.8	14.7	66.7	59.4
8	18.6	21.4	14.6	67.2	58.9
9	18.0	20.3	11.9	67.3	57.4

The experimental value is included for comparison.

We calculated the products and transition states for both pathways (Scheme 1) for compounds **1**−**9** (Figure 1) on the Becke3LYP/6-31G(d) level of theory (**BS1**); relative energies are shown in Table 1. On the higher level of theory (**BS2**), only the transition states have been optimized. The results are given in Table 2.

The experimental study[7a] was designed to study the steric and electronic influence of substituents on the oxidation rate. This is true for acrylic acid **1** with a delocalized electronic structure compared to vinylacetic acid **2** and 4-pentenoic acid **3**, where the double bond is localized with increasing distance to the carboxylic group. For compounds **4**−**9** the situation is more complicated because the substituents show a steric as well as an electronic effect. Additionally the effects are rather small; the experimental free activation energies lie within a narrow range of 17.0 to 18.6 kcal/mol for the various species.

For the unsubstituted, terminally unsaturated carboxylic acids **1**−**3** the experimental $\Delta G^{\ddagger}$ values show a similar trend compared to the calculated values for the (3 + 2) pathway. The activation energy needed to oxidize **1** is significantly lower, while **2** requires a higher activation energy than **3**.

We have computed the transition states on the double-ξ and triple-ξ level of theory to ensure that the choice of basis set has no major influence on the results.

The calculated transition states for compounds **1**−**3** show the largest disagreement between experimental and **BS2** computed value with 4.2 kcal/mol for $\mathbf{2_{TS}}$ (largest deviation) and 3.7 kcal/mol for $\mathbf{3_{TS}}$. It is remarkable that $\mathbf{1_{TS}}$ is the only case where the free activation energy was underestimated (by 1.4 kcal/mol). This result was unexpected, and we investigated the influence of the basis set as well as the molecular orbitals of $\mathbf{1_{TS}}$ and $\mathbf{2_{TS}}$.

Table 2 demonstrates that the computed triple-ξ values show less deviation from experiment compared to the double-ξ calculations, but also that the mechanistic answer is not dependent on the basis set used.

The X-ray structure of permanganate[12] was used to evaluate the DFT-calculated geometries of permanganate. The calculated bond length of 1.600 (**BS1**) and 1.601 (**BS2**) are both in excellent agreement with published X-ray data.

The geometries of the transition states differ significantly. While a rather symmetrical transition state is calculated for $\mathbf{2_{TS}}$ and $\mathbf{3_{TS}}$ with bond lengths of 2.05/2.06 Å ($\mathbf{2_{TS}}$) and 2.04/2.09 Å ($\mathbf{3_{TS}}$) for the forming bonds between the permanganate oxygens and the alkene carbons, $\mathbf{1_{TS}}$ shows an unsymmetrical, but still concerted transition state with calculated bond lengths of 2.29 and 1.90 Å. Coordinates of all geometries are given in the Supporting Information.

One would expect that the longer carbon chain of **2** compared to **1** leads to a difference in the transition state. But it is interesting to note that the distance between the carbonyl oxygen of the carboxylic group and the closest permanganate oxygen is almost identical in $\mathbf{1_{TS}}$ (3.33 Å) and $\mathbf{2_{TS}}$ (3.32 Å). The distance for $\mathbf{1_{TS}}$ should be a lot smaller, but the system avoids the repulsion, elongating one of the forming bonds.

Figure 2 shows the plot of the highest occupied molecular orbitals (HOMO) of $\mathbf{1_{TS}}$ and $\mathbf{2_{TS}}$. The plot of $\mathbf{1_{TS}}$ clearly shows the conjugation and the interaction between the oxygen lone pairs of the carboxylic group and the permanganate oxygens leading to the unsymmetry of the transition state. Energetically this repulsive interaction does not seem to be significant, the transition state $\mathbf{1_{TS}}$ is still calculated to have the lowest free activation barrier. CH_2 groups isolate the double bonds from the acid group in compounds **2** and **3**, inhibiting the conjugation. The symmetrical transition states $\mathbf{2_{TS}}$ and $\mathbf{3_{TS}}$ are very similar to the transition state calculated for the permanganate oxidation of ethene,[6b] indicating that the substitutent does not play a major role. The plot of $\mathbf{2_{TS}}$ shows how the CH_2 group shuts down the overlap and the conjugation.

Substrates **4**−**9** were chosen by Freeman[7a] to study the influence of steric bulk on the free activation energy. As discussed before, the substituents also show an electronic effect, and it is hard to separate both effects, but at least some comparisons can be made, e.g., for *trans*-crotonic acid **4** and 4,4-dimethyl-*trans*-2-pentenoic acid **9**. The steric bulk of the *tert*-butyl group compared to a methyl group should by far be more important than the difference in the electronic effect.

As can be seen from Tables 1 and 2, the activation energy increases slightly with the number of substituents. Monosubstitution independent of the position (**4**, **5**, **9**) results in activation energies of +18.3 to +20.3 kcal/mol ($\mathbf{4_{TS}}$, $\mathbf{5_{TS}}$, $\mathbf{9_{TS}}$). It is interesting to note that for methacrylic acid **4** and *trans*-crotonic acid **5** the position of the substituent does not influence the calculated activation energy ($\mathbf{4_{TS}}$, $\mathbf{5_{TS}}$).

Tiglic acid **6** was measured to have the lowest free activation energy, while 3-methylcrotonic acid **7** and 2,3-dimethylcrotonic acid **8** were experimentally found to require the highest activation energies. α,α-Disubstitution seems to have a large effect on the experimental rate constants. This is reproduced by the **BS2** calculated transition states, which have significantly higher free activation energies compared to those calculated for $\mathbf{4_{TS}}$−$\mathbf{6_{TS}}$. The calculated $\Delta\Delta G^{\ddagger}$ for the di- and trisubstituted alkenes ($\mathbf{7_{TS}}$ and $\mathbf{8_{TS}}$ compared to $\mathbf{6_{TS}}$) is 2.2 and 1.8 kcal/mol, respectively.

The geometries of the transition states of $\mathbf{4_{TS}}$−$\mathbf{9_{TS}}$ are similar regardless of the number of substituents. All transition states are very unsymmetrical, but concerted. The bond lengths of the C−O forming bonds do not change significantly, whether the substituent is a methyl group in α-position ($\mathbf{5_{TS}}$, 2.30/1.91 Å), β-position ($\mathbf{4_{TS}}$, 2.31/1.92 Å), or a *tert*-butyl group ($\mathbf{9_{TS}}$, 2.29/1.93 Å).

Even three methyl groups as in $\mathbf{8_{TS}}$ do not distort the geometry more than what was observed for $\mathbf{1_{TS}}$. It can be concluded that the conjugative effect and the repulsive

(12) Palenik, G. J. *Inorg. Chem.* **1967**, *6*, 503.

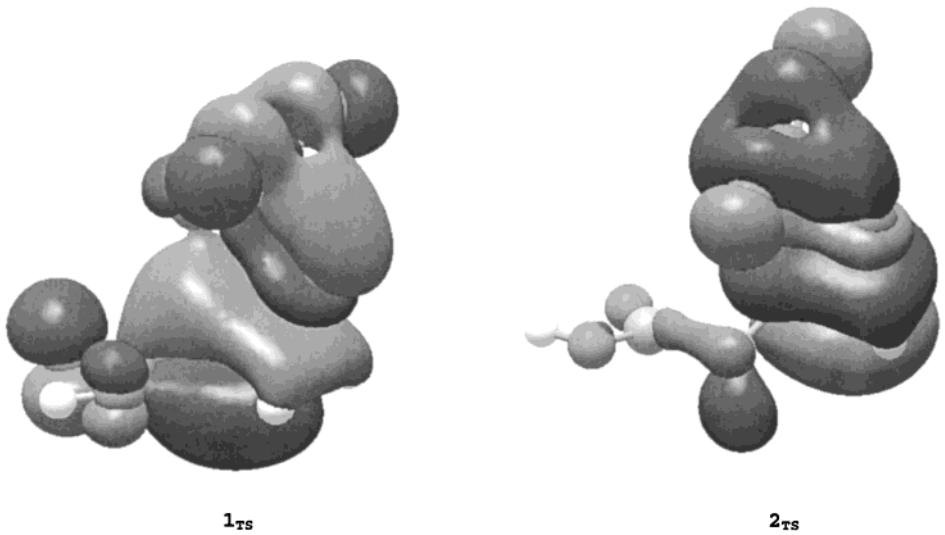

Figure 2. Highest occupied molecular orbitals (HOMO) of transition states $\mathbf{1}_{TS}$ and $\mathbf{2}_{TS}$.

interaction are more important than the steric bulk. Certainly the interaction is weaker in solution, where the negative charge of the permanganate ion is going to be solvated, especially in aqueous solution. Therefore we conducted solvens calculations using the PCM model of Tomasi and co-workers. As can be seen from Table 2, the (3 + 2) pathway is still hugely favored, and the activation energies for the solvated (3 + 2) transition states are in reasonable agreement, although they are in general lower than the experimental values with the exception of compound **8**. Compared to the gas-phase calculations, the deviations are much smaller.

The products have only been calculated by **BS1**. The numbers shown in Table 1 demonstrate that the (3 + 2) product is hugely favored and that a larger basis set will not change the mechanistic answer. The formation of the (3 + 2) products is rather exergonic with values ranging from −30.0 kcal/mol to −38.1 kcal/mol (Table 1).

The transition states have been calculated with the smaller basis **BS1** and the larger basis **BS2** (Table 2). The rmsd between calculated and experimental values is smaller for the larger basis, and the calculated free energy of activation for the (3 + 2) transition states $\mathbf{1}_{TS}$−$\mathbf{9}_{TS}$ yields values from +15.7 kcal/mol up to +22.0 kcal/mol for the 9 different substrates. These values differ significantly from those calculated for the (2 + 2) pathway!

The stepwise (2 + 2) mechanism proceeds via a metallaoxetane transition state and a transient metallaoxetane species ((2 + 2) product) which is supposed to rearrange to the (3 + 2) product (Scheme 1). For all nine compounds, this pathway requires very high free activation energies ranging from 61.5 kcal/mol to 67.3 kcal/mol (**BS2**, Table 2).

The (2 + 2) products are calculated to be endergonic with energies of +24.7 kcal/mol to +33.6 kcal/mol (**BS1**, Table 1).

The endergonic formation of a metallaoxetane product via a transition state that is on the average 40 kcal/mol higher in energy as the transition state of the competing pathway which leads to a exergonic product is highly improbable and will not be significantly populated.

Figure 3 shows a comparison of the experimental values of activation versus the (3 + 2) and (2 + 2) transition state. All calculated activation energies for the (3 + 2) TS are in close proximity to the experimentally observed values, while the smallest difference between the (2 + 2) transition states and the experimental values is 44.4 kcal/mol. This energy difference is similar to the one observed for the OsO_4 dihydroxylation reaction.[5,6]

For osmium tetraoxide the rearrangement transition state turned out to be even more unfavorable. As discussed above the pathway via the (2 + 2) transition state and the metallaoxetane is not going to be significantly populated competing with a pathway via the (3 + 2) transition state. These results suggests that the mechanism of the permanganate oxidation proceeds through a (3 + 2) TS, leading to a manganate ester which then is hydrolyzed to *cis*-diols.

Additionally the thermodynamically most stable species is the (3 + 2) product which is exergonic by more than 30 kcal/mol. Therefore we did not investigate the rearrangement transition states leading from the metallaoxetane to the cyclic ester product.

B3LYP/6-31G(d) has shown in many cases[13] that it is a reliable combination of functional and basis set for organometallic compounds. But sometimes a larger basis (B3LYP/6-311+G(d,p)) is needed to evaluate a flat potential energy surface, e.g., to compute the C−H abstraction reaction of permanganate with toluene and methane.[14] We evaluated the influence of the basis set, but for the systems described here the choice of basis set is less critical. As expected the deviation of experimental and calculated $\Delta G^{\ddagger}$ values is smaller for **BS2**, but also **BS1** gave good results as can be seen in Figure 4. It shows the influence of the basis set on the ground and transition state geometries of vinylacetic acid **2**. Values for **BS2** are given in parentheses. We chose vinylacetic acid **2** to discuss the basis set effect on the geometry (Figure 4); the results for acrylic acid **1** are similar.

The largest deviations would be expected for the forming bonds, but these are very small for the (3 + 2) transition state. Most bond lengths do not change; only some deviate by 0.01 Å. The dihedral angle Mn−O−C−C decreases with increasing level of theory (from **BS1** to

(13) Frenking, G.; Antes, I.; Boehme, M.; Dapprich, S.; Ehlers, A. W.; Jonas, V.; Neuhaus, A.; Otto, M.; Stegmann, R.; Veldkamp, A.; Vyboishchikov, S. F. *Reviews in Computational Chemistry*; Lipkowitz, K. B., Boyd, D. B., Eds.; VCH: New York, Vol. 8, 1996; pp 63−144.

(14) Strassner, T.; Houk, K. N. *J. Am. Chem. Soc.* **2000**, *122*, 7821.

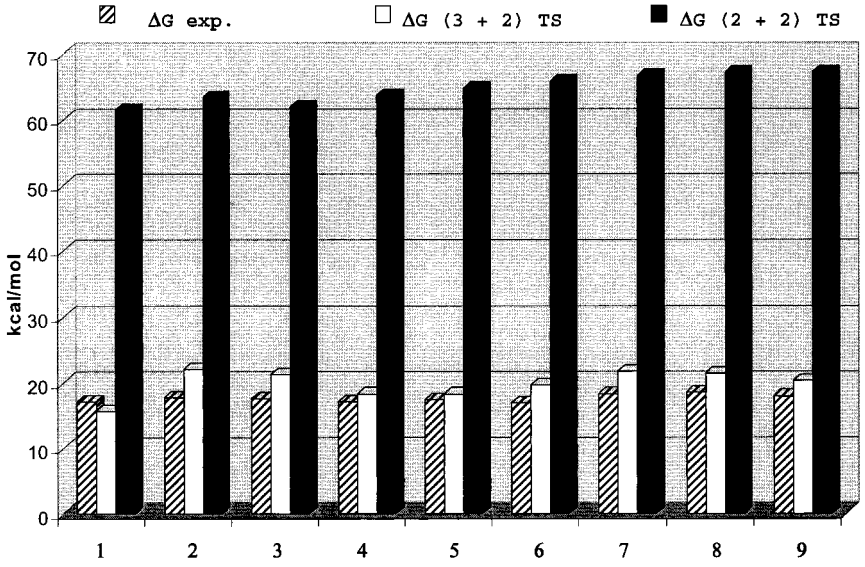

Figure 3. Chart of calculated free energies for the (3 + 2) and (2 + 2) transition states vs the experimentally observed value of compounds **1**−**9** in kcal/mol (**BS2**).

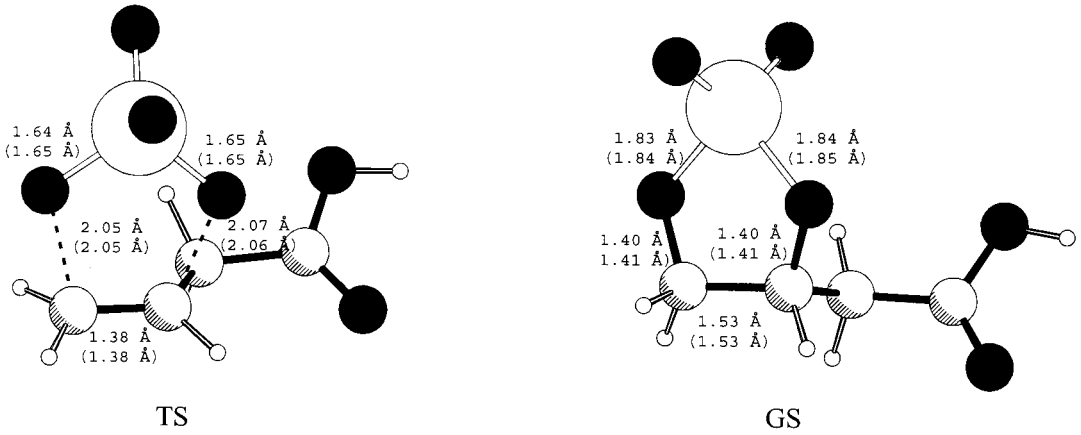

Figure 4. Basis set effect on the transition state (TS) and ground state (GS) geometries for the (3 + 2) addition of vinylacetic acid **2**. Values for **BS2** are given in parentheses.

BS2) from −6.7° to −3.6°, indicating more overlap of the carbon and oxygen orbitals. The geometry of the cyclic ester product is very similar as can be seen from Figure 4. No considerable effect of the basis set can be found in the geometries. The maximum deviation of the bond lengths is again 0.01 Å; the Mn−O−C−C angle changes from −32.4° to −28.6°.

Energetically, the triple-ζ basis set II leads to an increase of $\Delta G^{\ddagger}$ for the (3 + 2) transition states by 4.9 kcal/mol for $\mathbf{1}_{TS}$ and 4.3 kcal/mol for $\mathbf{2}_{TS}$ (Table 2). This leads to a better agreement between experimental and calculated value for $\mathbf{1}_{TS}$, but overestimates the free activation energy of $\mathbf{2}_{TS}$.

In general, the agreement between experimental and calculated value over (3 + 2) transition states for all nine compounds is better for the higher basis set, the calculated rmsd drops from 2.58 kcal/mol (**BS1**) to 1.87 kcal/mol (**BS2**).

For the (2 + 2) transition states calculated by **BS2**, we observe even higher free activation energies, which further increase the gap between calculated and experimental values.

Therefore we can conclude that density functional theory calculations strongly favor the (3 + 2) pathway for permanganate oxidations. No direct interaction of the transition metal with the alkene is necessary to explain the kinetic data. The triple-ζ basis set reduces the rmsd between experimental and calculated values, but has only little influence on the geometries.

Acknowledgment. We are indebted to Prof. W. A. Herrmann for his generous and continuous support of our work. We are grateful to the Leibniz-Rechenzentrum München for providing the necessary computer time. Support from the Dr. Karl-Wamsler-Stiftung and Leonhard-Lorenz-Stiftung is gratefully acknowledged.

Supporting Information Available: The *xyz*-coordinates of all educts, transition states, and ground states for **BS1** and **BS2**. This material is available free of charge via the Internet at http://pubs.acs.org.

JO000575E